ISSN (Print) 1226-1750
ISSN (Online) 2233-6656
Journal of Magnetics 27(4), 373-378 (2022) https://doi.org/10.4283/JMAG.2022.27.4.373

Effect of Heat Treatments on Magnetic Properties and Thermal Expansion Behavior in Two Distinct Types of Fe-Ni Invar Alloys

Lin Huang[1]*, Tingwen Guo[1], Yongjian Zhou[1], Dong Han[2], Yu Gu[2], Cheng Song[1], and Feng Pan[1]

[1]*Country Key Laboratory of Advanced Materials (MOE), School of Materials Science and Engineering, Tsinghua University, Beijing, China*
[2]*Shanxi Taigang Stainless Steel Co., Ltd, Taiyuan, China*

(Received 20 September 2022, Received in final form 6 December 2022, Accepted 7 December 2022)

The casting process of Fe-Ni Invar alloy could drastically affect magnetic properties and thermal expansion. We have observed analogous trends of saturation magnetization and thermal expansion coefficient in two distinct types of casted samples, as we perform post-annealing at different temperatures. X-ray diffraction measurements show that all the alloys remain in the same face-centered cubic structure after different heat treatments without phase transformation. With the help of X-ray diffraction and differential thermal analysis, we have inferred that these changes in properties might be induced by magnetic lattice transitions and analyzed the possible reason for property differences in samples. This work delivers a perspective on the relationships between thermal expansion, magnetic properties, and heat treatments, which could help to improve the industrial assembly line design.

Keywords : invar alloy, magnetization, coefficient of thermal expansion

1. Introduction

The Alloys of the Fe-Ni system with nickel content of around 36 wt% are named as Fe-36Ni Invar alloys, which is are well known for their extremely low coefficient of thermal expansion (CTE) around room temperature [1-4]. It has been used in designing and developing high precision mechanical instruments, the electronic industry, aerospace technology, large-size cryogenic liquid containers, and high-definition color displays [5-8]. $Fe_{64}Ni_{36}$ has a face-centered cubic (fcc) structure around room temperature. In addition to the well-known CTE anomaly, invar alloys also exhibit anomalous features in the temperature dependencies of the magnetization (M_s), Curie temperature (T_c), coercivity (H_c), and atomic volume [9-11]. It is generally believed that the low thermal expansion coefficient of these alloys is due to the cancellation of lattice expansion by large positive spontaneous volume magnetostriction below the Curie temperature [12-14]. And the study of the Invar effect has become an important topic in the study of metal magnetism, extensive and in-depth studies have been carried out from both theoretical and experimental aspects [15-17].

In this regard, it seems essential to focus attention on the effect of spontaneous volume magnetostriction and Curie temperature on thermal expansion in the structure of alloys. Although there are too many factors that can affect the Invar effect, for instance, there may exist a large amount of defects in the material that the internal stress may be released and the texture should be strengthened after annealing [18, 19], a full understanding is still being studied. It has been reported that freezing processing technology increases the internal defects of Fe-36Ni alloy, reduces the density, destroys the short-range atomic ordering degree, affects the spontaneous magnetization and magnetostriction coefficient of the alloy, and finally reduces the thermal expansion coefficient even to negative [20]. Here, we present the temperature-dependent magnetic properties and thermal expansion of industrially casting processed Invar alloys, and pave a new perspective for an economical method of alloy preparation. The main goal of this work can be formulated as follows: to find out which particular type of the Fe–Ni alloy is responsible for the appearance of the invar effects, in order to have a clear idea of the heat

*Corresponding author: Tel: +86-185-1328-5122
e-mail: lhuang2020@mail.tsinghua.edu.cn

treatment needed to obtain the best properties.

2. Materials and Methods

The materials used in this work are prepared by Shanxi Taigang Stainless Steel Co., Ltd. The vertical bending continuous casting machine was used for continuous casting of Invar alloy, in which the molten steel is superheated by 20-40 °C in the tundish, the electric stirring parameters of the mold are 400A, 5 Hz, 15s, and in the end straightens at 860-900 °C. Method 1 is the sample with the continuous casting process, Method 2 is the sample with the continuous casting process and annealing temperature at 900 °C treatment for 3 hours, then it cools naturally. The chemical composition of the raw sample is shown in Table 1. Based on the composition, it is a typical Fe-36Ni alloy (hereafter referred to as Raw sample). Then, invar alloy materials of Method 1 and Method 2 are annealed at different temperatures of 300 (sample T300), 500 (T500), 600 (T600), and 1000 °C (T1000) for 2 hours and then underwent furnace cooling, respectively. X-ray diffraction (XRD) spectra with Cu Kα x-ray source are used to characterize the microstructures after various heat treatments. Magnetic properties are characterized by a superconducting quantum interference device (SQUID), the vibrating sample magnetometer (VSM). The differential thermal analysis (DTA) was measured by thermogravimetric-differential thermal analysis (No. STA499F3 NETZSCH-Gerätebau GmbH), samples are measured by thermogravimetric differential thermal analysis (TG-DTA) in an inert atmosphere of argon, at the temperature range from 50 °C to 1000 °C. The coefficient of thermal expansion value is the average value of the measured temperature range from 20-100 °C (heating start temperature is 10 °C and end temperature is 120 °C), and the temperature ramp is 5 °C/min. Moreover, we used the Cuboid shape samples with 10 × 10 × 5 mm^3, each sample was repeated three times to extract the coefficient of thermal expansion.

Table 1. Composition of the cold-drawn Invar Fe-Ni alloy wire with wt% ≥ 0.01%.

C	Si	Mn	Al	Cu	Ni	Fe
0.0137	0.1174	0.274	0.01	0.011	35.95	63.624

3. Results and Discussion

Figure 1 shows room temperature XRD spectra of Invar-alloys (Sample: Raw, T300, T500, T6000, and

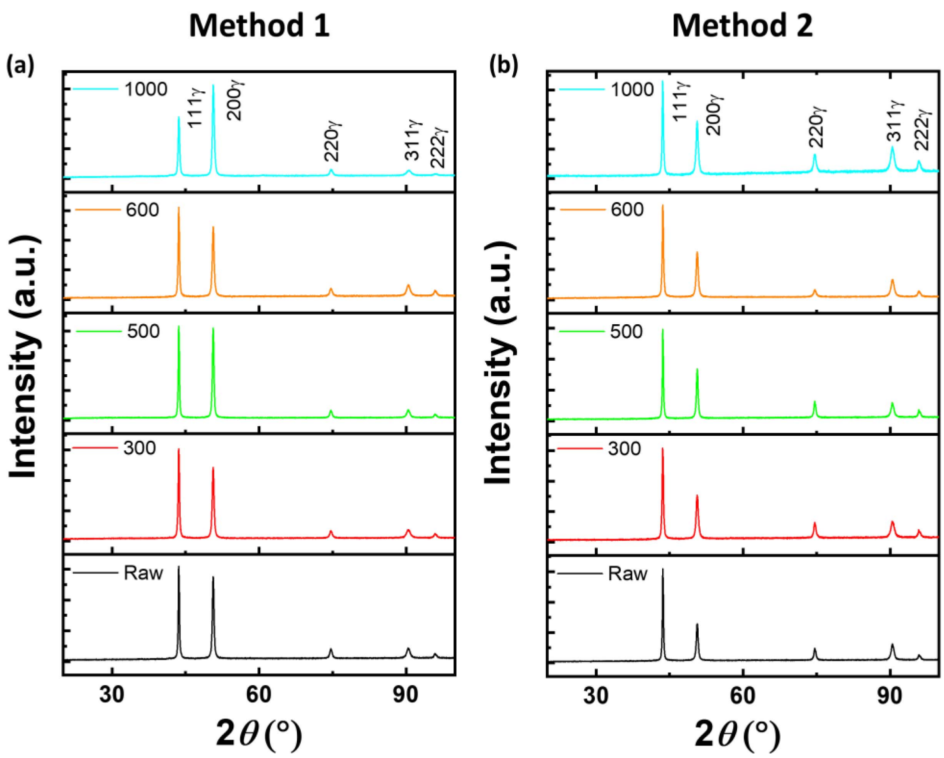

Fig. 1. (Color online) XRD spectra at room temperature for Invar alloy sample Method1 (a) and Method 2 (b) with various heat treatment conditions: Raw, T300, T500, T600, and T1000, respectively.

T1000) in the 2θ range of $30^{o} \leq 2\theta \leq 100^{o}$ for sample Method 1 (Fig. 1(a)) and sample Method 2 (Fig. 1(b)). From the continuous casting, Figure 1 shows room temperature XRD spectra of Invar-alloys (Sample: Raw, T300, T500, T600, and T1000) in the 2θ range of $30^{o} \leq 2\theta \leq 100^{o}$ for sample Method 1 (Fig. 1(a)) and sample Method 2 (Fig. 1(b)). From the continuous casting method, it is indicated that the rolling texture is formed. All the Invar-alloy samples show the signal phase fcc structure at room temperature [21] and no phase transition is formed at the heat treatment temperature range which is quite well compared with the structure of Raw Invar-alloy. However, sample Method 1 annealed at 1000 °C, the intensity of peak (111γ) and peak (200γ) shows significant decrease and increase, respectively. And other intensities of peaks (peak position: (220γ), (311γ), and (222γ)) almost remain the same compared to the Raw sample. For sample Method 2, when annealing at a higher temperature, the strength of all the peaks rises slightly compared the Raw sample. It indicates that the quality of crystallization improves after high-temperature annealing, which could also take an effect on magnetism with different heat treatment conditions. Here, we focus on the magnetic properties and the coefficients of thermal expansion with various heat treatment conditions.

We also investigate the magnetic properties of Invar-alloys with different post-annealing heat treatment conditions. The magnetic hysteresis loops (*M–H* loops) in Fig. 2 are measured at room temperature. All of the *M–H* loops demonstrate strong soft magnetic properties with small coercive field (H_c) (smaller than 10 Oe) in H_c extracted from the *M–H* loops as a function of heat treatment temperature (*T*) is shown for Method 1 (Fig. 2(a)) and Method 2 (Fig. (b)). All the samples showed a soft magnetic property, and the H_c appears to be very small (smaller than 10 Oe). The coercivity comes from the irreversible magnetization process, the main factor causing the irreversible magnetization mechanism is the magnetic anisotropy (including intrinsic and strain-caused magneto-crystalline anisotropy) in the material, as well as impurities, pores, defects, and other factors, which also affect the magnitude of coercivity. Among the magnetic properties, the coercivity force is most strongly affected by grain size.

Moreover, the differential thermal analysis (DTA) measured at the temperature range from 50 °C to 1000 °C, is plotted in Fig. 3. Endothermic peaks for both samples appear at least twice, and the first peak between 350 and 500 °C is markedly different for samples, while the second peaks both appear at around 900 °C. In rolling

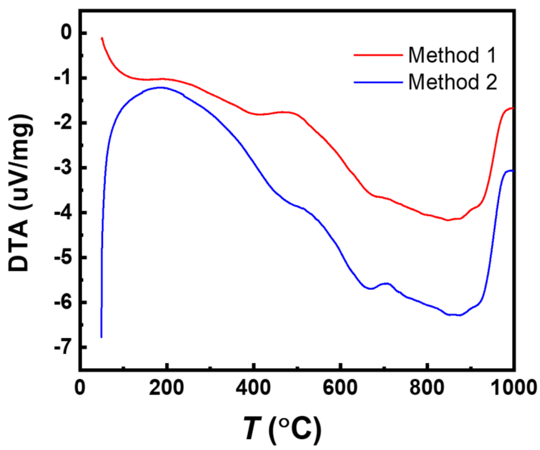

Fig. 3. (Color online) Differential thermal analysis (DTA) as the function of temperature (range from 50 °C to 1000 °C) for both samples: Method 1 and Method 2.

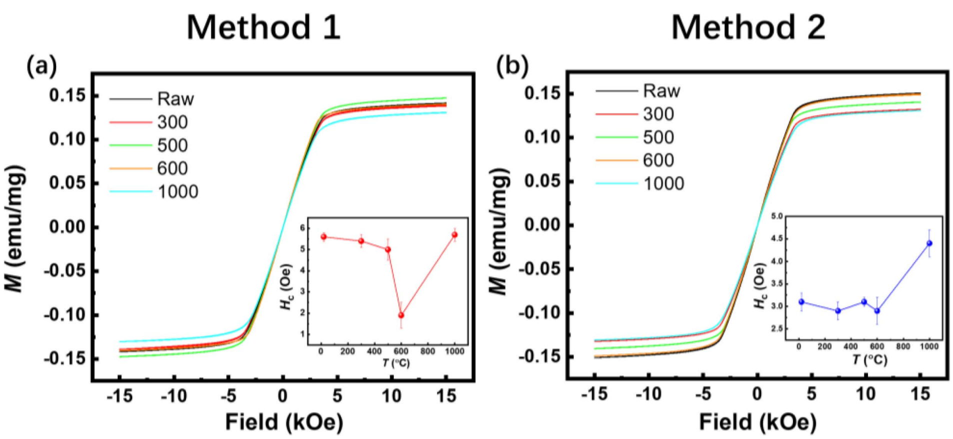

Fig. 2. (Color online) *M–H* loops of Invar alloy wires with various heat treatment conditions for Method 1 (a) and Method 2 (b), and the H_c as a function of heat treatment temperature (T) extracted from M–H loops shown in the inset of (a) and (b).

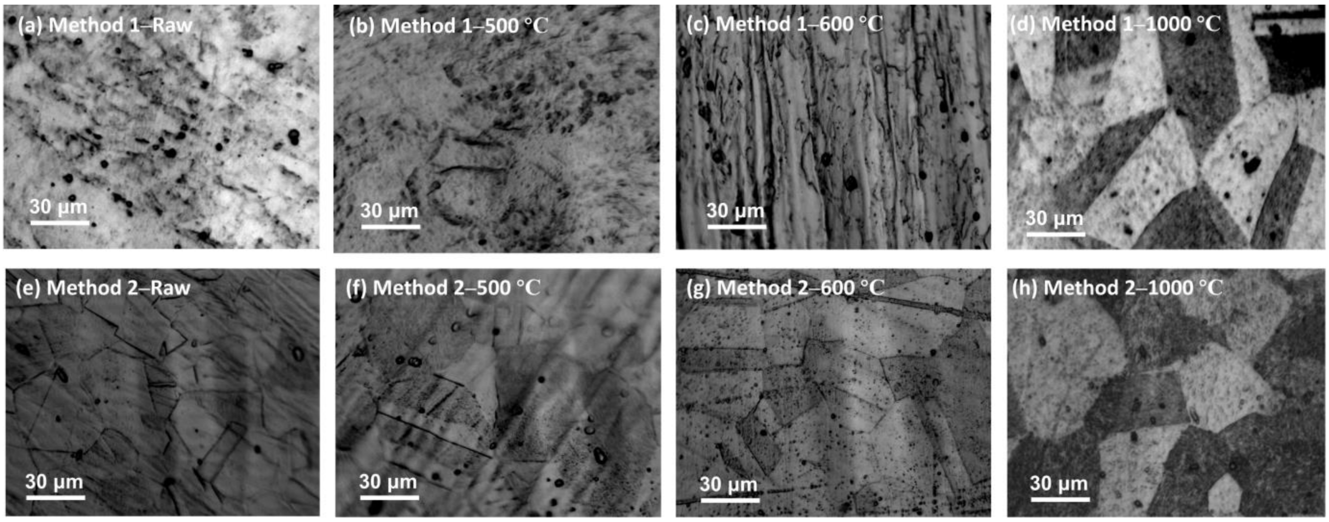

Fig. 4. Metallographic structure of samples treated with different heat treatment processes for Method 1 and Method 2.

textures, internal stress could be released by annealing. Through comparison, it is implied that the lower Curie-temperature sample has a lower temperature of recovery, but the re-crystallization temperature remains the same. This argument is qualitatively reasonable, since the recovery process releases internal stress within grains, so it is strongly affected by magnetostriction. For the recrystallization, the temperature is not affected because the magnetostriction has already been released, and the nucleation of new grains is almost irrelevant to magnetism.

Then after Method 1 annealing at 500 °C (Fig. 4(b)), the microstructure after annealing is fine. The grain is coarse and accompanied by a small number of annealing twins, but the uniformity has been greatly improved. When Method 1 annealed at 600 °C (Fig. 4(c)), the structure appears like a plate strip, significantly different from the microstructure shown in Fig.4 (a) and Fig. 4(b). After annealing at 1000 °C (Fig. 4(d)), the fully re-crystallized structure is formed by equiaxed grains, and the interlayer fault energy of the invar alloy is lowered during the annealing process. According to Fig. 2, it can be explained that the coercivity decreases with increasing grain size when the temperature is lower than 600 °C (as shown in Fig. 4(a) and Fig. 4(b)). When the annealing temperature is 600 °C (Fig. 4(c)) and the structure appears like a plate strip, significantly different from the microstructure shown in Fig. 4(a) and Fig. 4(b), grain sizes corresponding to minimum coercivity corresponding to single domain sizes.

At the same time, it can be seen from Fig. 4(e) that after holding at 900 °C for 3 hours (Method 2), the recrystallization process has basically been completed and the new grains have been completely close to each other, that is, the storage energy caused by deformation has basically been released. With the increase of annealing temperature (Fig. 4(f) and Fig. 4(g)), the grain size increases gradually, indicating that the grains recrystallized and grew up. When the annealing temperature is increased to 1000 °C (Fig. 4(h)), the grain coarsening is obvious, because the grain size after annealing mainly depends on the degree of deformation and annealing temperature. When the shape variable is constant, the higher the temperature, the larger the grain size.

The saturation magnetization (M_s) and coefficient of thermal expansion (α) with different heat treatment conditions with sample Method 1 and Method 2 are shown in Fig. 5(a) and Fig. 5(b), respectively. With the increasing annealing temperature range from 300 to 1000 °C, T500 shows the highest M_s for sample Method 1 and T600 shows the highest M_s for sample Method 2. Compared with the continuous casting process without annealing (Method 1), the continuous casting process with annealing at 900 °C (Method 2) shifts the value of M_s. We have observed that with the variation of annealing temperature, the change of thermal expansion coefficient shows the similar trend of the saturation magnetization. The maximum α appears in T500 and T600 of sample Method 1 and Method 2 (Fig. 5(b)), respectively. It is found that the magnetic properties play a role in the coefficient of thermal expansion for Invar alloys. The thermal expansion value α is proportional to the M_s as well as spontaneous volume magnetostriction λ. The fact that we can estimate that the spontaneous volume magnetostriction λ is proportional to M_s is consistent with the research, as Ref. [22] showed. The spontaneous volume magnetostriction λ is proportional to the square of the

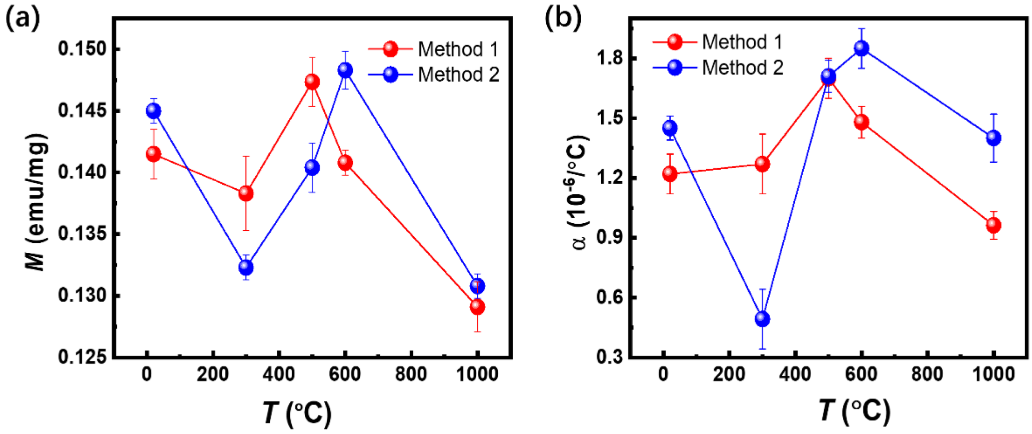

Fig. 5. (Color online) Saturation magnetization (M_s) (a) and coefficient of thermal expansion (α). (b) as the function of the heat treatment temperature (T) for sample Method 1 and Method 2, respectively.

magnetization M^2 as $\lambda \approx \kappa C^{band} M^2$, where C^{band} is the magneto-volume coupling constant [23]. It is believed that magnetostriction has a certain effect on the thermal expansion coefficient, which cancels out the normal lattice contraction, resulting in an almost zero expansion rate at room temperature.

It is indicated that the change of λ is related to the molecular field, and thus could be analyzed via the measurement of Curie temperature. Therefore, M–T measurements at the temperature range from 300 to 800 °C are given in Fig. 6(a) under a 50 Oe external magnetic field. The derivative of the magnetization (dM/dT) is given in Fig. 6(b), and the minimum value of dM/dT corresponds to Curie-temperature (T_c). Comparing the T_c

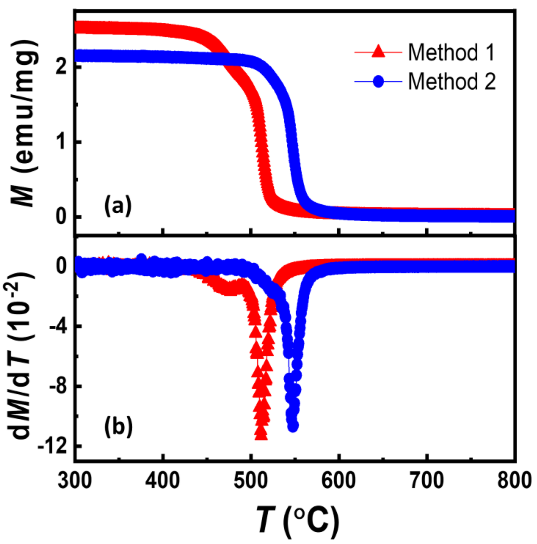

Fig. 6. (Color online) (a) $M(T)$ measurements of the Invar alloys (Method 1 and Method 2). (b) Derivative of the magnetization (dM/dT).

of sample Method 1 and Method 2, where the red points correspond to Method 1 with the lowest $T_c \approx 510$ °C, and the T_c of Method 2 (blue points) is improved to 550 °C.

It reveals that after annealing at 900 °C for 3 hours (Method 2), the T_c shifts to a higher temperature compared to Method 1, as well as the saturation magnetization and coefficient of thermal expansion. The atomic magnetic moment of ferromagnetic material receives the action of the molecular field inside the material, which leads to spontaneous magnetization, that is, in the absence of an external magnetic field the ordered arrangement of microscopic magnetic moments is still presented. In the Invar alloys, with the increase in temperature, the energy of atomic thermal motion increases, which gradually destroys the ordered arrangement of atomic magnetic moments in the magnetic material. When the temperature rises to Curie temperature, the energy of thermal motion is equal to the energy of exchange, the ordered arrangement of atomic magnetic moments does not exist, and the strong magnetism disappears, presenting paramagnetism. As the magnetic moment per atom of ferromagnetic material in both materials is fixed as $gS\mu_B$, the spontaneous magnetization of the atomic magnetic moment will be disturbed by the thermal motion of ferromagnetic atoms during the annealing process, and the atomic magnetic moment will be affected by the internal molecular field H_m, where $H_m = \lambda M$ and λ is the molecular constant coefficient. Under the effect of molecular field H_m, atomic magnetic moments are arranged in parallel due to spontaneous magnetization, and the interaction energy between molecular field and atomic magnetic moments is $H_m g S \mu_B$. When the temperature reaches Curie-temperature T_c, the thermal motion energy of atoms is equivalent to the energy of spontaneous magnetization, which can be expressed as $kT_c = H_m g S \mu_B$, where g is Lande factor, S is the spin moment, k is Boltzmann constant and μ_B is Bohr magneton [24]. Thus, Curie-temperature makes it fluctuate between different orientations, and the Curie-temperature T_c in ferromagnetic alloys marks the breakdown of the long-range magnetic order. The magnetic moment of each atom is itself a thermal average, as the competition between the exchange, thus the relationship between curie temperature and magnetic order can be explained. On the other hand, we should also note that the change of the coupling energy between molecular field and magnetization represents a change in exchange interaction Δ of electrons. The splitting energy 2Δ between majority-spin and minority-spin electron bands would change, which eventually results in the change of magnetization and Curie temperature for samples. This argument is consistent with the itinerant electron magnetism theory. The change of molecular field results in the change of magnetic properties, thermal expansion coefficient, and Curie temperature of Invar alloys.

4. Conclusions

We have investigated the effect of magnetic properties on the coefficient of thermal expansion with different heat treatment conditions for two different casting processes (continuous casting and continuous casting after 900 °C annealings) Fe-36Ni Invar alloys. Our results show that: (1) phases kept unchanged with different heat treatment conditions; (2) After different heat treatments, the saturation magnetization and coefficient of thermal expansion show a similar trend for the various heat treatment conditions; (3) The heat treatment of annealing results in a change in the molecular field of the sample continuous casting and continuous casting after 900 °C annealing, and atomic magnetic moments are arranged in parallel due to spontaneous magnetization, and the interaction energy between molecular field and atomic magnetic moments, the change of molecular field results in the change of magnetic properties, thermal expansion coefficient and Curie temperature of Invar alloys. We conclude that after different heat treatment conditions for Invar alloys, the magnetic properties play a role in obtaining a low coefficient of thermal expansion without phase transition. This has potential application value for the decoration of standard parts and the external compensation of clocks and watches.

Acknowledgments

This research was supported by Department of science and technology of Shanxi Province (Grant No. 20201101011).

References

[1] J. R. Davis, Alloying: understanding the basics. Ohio: ASM international; 2001.
[2] M. V. Schilfgaarde, I. A. Abrikosov, and B. Johansson, Nature **400**, 46 (1999).
[3] C. E. Guillaume, Nature **131**, 658 (1933).
[4] A. Sahoo and V. R. R. Medicherla, Mater. Today: Proc. **43**, 2242 (2021).
[5] Y. Liu, L. Liu, J. Li, B. Shen, and W. Hu, J. Alloy. Compd. **478**, 750 (2009).
[6] I. Tabakovic, V. Inturi, J. Thurn, and M. Kief, Electrochimica. Acta. **55**, 6749 (2010).
[7] W. Pepperhoff and M. Acet, Springer, Berlin (2001) pp 106.
[8] S. J. Park, S. H. Jo, S. Oh, Y.-S. Oh, S.-J. Kim, H. W. Lee, S. H. Kang, Y.-H. Moon, and J. Jung, Mater. Design. **217**, 110631 (2022).
[9] S. N. Khanna and S. Linderoth, Phys. Rev. Lett. **67**, 742 (1991).
[10] L. Yiping, G. C. Hadjipanayis, C. M. Sorensen, and K. J. Klabunde, J. Magn. Magn. Mater. **104**, 1545 (1992).
[11] J. P. Chen, C. M. Sorenson, K. J. Klabunde, G. C. Hadjipanayis, E. Devlin, and A. Kostikas, Phys. Rev. B **54**, 9288 (1996).
[12] A. Iwase, Y. Hamatani, Y. Mukomoto, N. Ishikawa, Y. Chimi, T. Kambara, C. Muller, R. Neumann, and F. Ono, Nucl. Instr. and Meth. B. **209**, 323 (2003).
[13] Y. Matsushima, N. Q. Sun, H. Kanamitsu, M. Matsushita, A. Iwase, Y. Chimi, N. Ishikawa, T. Kambara, and F. Ono, J. Magn. Magn. Mater. **298**(1), 14 (2006).
[14] P. Goria, D. Martinez-Blanco, J. A. Blanco, and R. I. Smith, J. Alloys. Compd. **495**(2), 495 (2010).
[15] A. Vinogradov, S. Hashimoto, and V. I. Kopylov, Mater. Sci. Eng. A **355**, 277 (2003).
[16] T. Pan, J. Zhu, H. Su, and C. F. Yang, Rare Met. **34**, 776 (2015).
[17] L. Chen, J. F. Zhang, L. Zhang, and L. Meng, Int. J. Miner. Metall. Mater. **16**, 667 (2009).
[18] J. P. Yuan, D. Q. Yi, Z. M. Yu, Z. C. Huang, B. T. Wu, and X. Zhang, Heat Treat Met. **30**(2), 50 (2005).
[19] P. Z. Si and C. J. Choi, Metals, **8**, 28 (2018).
[20] J. Liu, Met. Funct. Mater. **14**(5), 33 (2007).
[21] A. Sajjad, B. Z. Amer, N. A. Muhammad, I. Ather, A. Shabbar, A. Naseeb, S. Muhammad, and A. K. Muhammad, J. Magn. Magn. Mater. **419**, 125 (2016).
[22] L. Huang, Y. Zhou, T. Guo, D. Han, Y. Gu, C. Song, and F. Pan, Materials **15**, 1504 (2022).
[23] M. Shiga, J. Phys. Soc. Jpn. **50**, 2573(1981).
[24] D. S. Dai and Qian, K. M. (Eds.) Ferromagnetism, Science Press (Version 2) Handbook; Science Press: Beijing, China (2017) pp 124-132.